First publ. in: Structure 8 (2000), pp. 585-592

A conserved structural motif for lipopolysaccharide recognition by procaryotic and eucaryotic proteins

Andrew D Ferguson[1,2], Wolfram Welte[1], Eckhard Hofmann[1], Buko Lindner[3], Otto Holst[3], James W Coulton[2] and Kay Diederichs[1]*

Background: Lipopolysaccharide (LPS), a lipoglycan from the outer membrane of Gram-negative bacteria, is an immunomodulatory molecule that stimulates the innate immune response. High levels of LPS cause excessive release of inflammatory mediators and are responsible for the septic shock syndrome. The interaction of LPS with its cognate binding proteins has not, as yet, been structurally elucidated.

Results: The X-ray crystallographic structure of LPS in complex with the integral outer membrane protein FhuA from *Escherichia coli* K-12 is reported. It is in accord with data obtained using mass spectroscopy and nuclear magnetic resonance. Most of the important hydrogen-bonding or electrostatic interactions with LPS are provided by eight positively charged residues of FhuA. Residues in a similar three-dimensional arrangement were searched for in all structurally known proteins using a fast template-matching algorithm, and a subset of four residues was identified that is common to known LPS-binding proteins.

Conclusions: These four residues, three of which form specific interactions with lipid A, appear to provide the structural basis of pattern recognition in the innate immune response. Their arrangement can serve to identify LPS-binding sites on proteins known to interact with LPS, and could serve as a template for molecular modeling of a LPS scavenger designed to reduce the septic shock syndrome.

Addresses: [1]Fakultät für Biologie, Universität Konstanz, M656, D-78457 Konstanz, Germany, [2]Department of Microbiology and Immunology, McGill University, 3775 University Street, Montreal, Quebec, Canada H3A 2B4 and [3]Forschungszentrum Borstel, Zentrum für Medizin und Biowissenschaften, Parkallee 1-45, D-23845 Borstel, Germany.

*Corresponding author.
E-mail: Kay.Diederichs@uni-konstanz.de

Key words: innate immune response, lipopolysaccharide, septic shock, siderophore-mediated iron acquisition, TonB-dependent receptor

Introduction

Lipopolysaccharide (LPS or endotoxin), a complex lipoglycan found exclusively in the outer membrane of Gram-negative bacteria [1–3], is a potent activator of the innate (nonclonal) immune system [4,5]. Low doses of LPS stimulate macrophages and neutrophils to produce cytokines and inflammatory mediators, thereby providing resistance to bacterial infections. High doses of LPS cause excessive release of inflammatory mediators and might lead to septic shock, a medical condition that is responsible for an estimated 200,000 deaths per year in the United States alone. Although some proteins have been identified as targets of LPS activity, detailed atomic interactions between the cognate residues on those targets and specific sites of LPS are unknown.

The objectives of our studies were to establish, using X-ray crystallography, the three-dimensional structure of LPS, to integrate LPS into the current model of the molecular architecture of the bacterial outer membrane (OM), and to identify characteristic patterns of protein–LPS interactions that derive from the crystal structure of a complex of LPS with an OM protein. Our target protein is FhuA, a ferric hydroxamate uptake receptor that is found on the surface of *Escherichia coli*. FhuA belongs to a family of proteins that mediates the active transport of siderophores including ferrichrome into Gram-negative bacteria [6]. We recently solved [7] the crystal structure of FhuAs that were isolated from two strains of *E. coli* K-12: strain AW740 (2.5 Å resolution) and strain DL41 (2.7 Å). FhuA consists of a C-terminal β barrel formed by 22 antiparallel transmembrane β strands and an N-terminal cork that fills the barrel interior. During the course of model building and structural refinement, we observed additional electron density proximal to the membrane-embedded region of the barrel. This electron density was modeled as a single LPS molecule, tentatively using the most abundant *E. coli* K-12 LPS chemotype [8].

LPS is composed of three covalently linked domains, which are differentiated by their genetic organization, biosynthetic pathways, chemical structures and biological features [8]. These domains are lipid A, a mostly invariant glycolipid that acts as an amphiphilic anchor in the OM (Figure 1); the core, a variable non-repeating heterooligosaccharide; and O antigen, an immunogenic highly variable repeating polysaccharide that extends into the external medium. The chemical composition and conformation of lipid A are determinants of its endotoxic activity

Figure 1

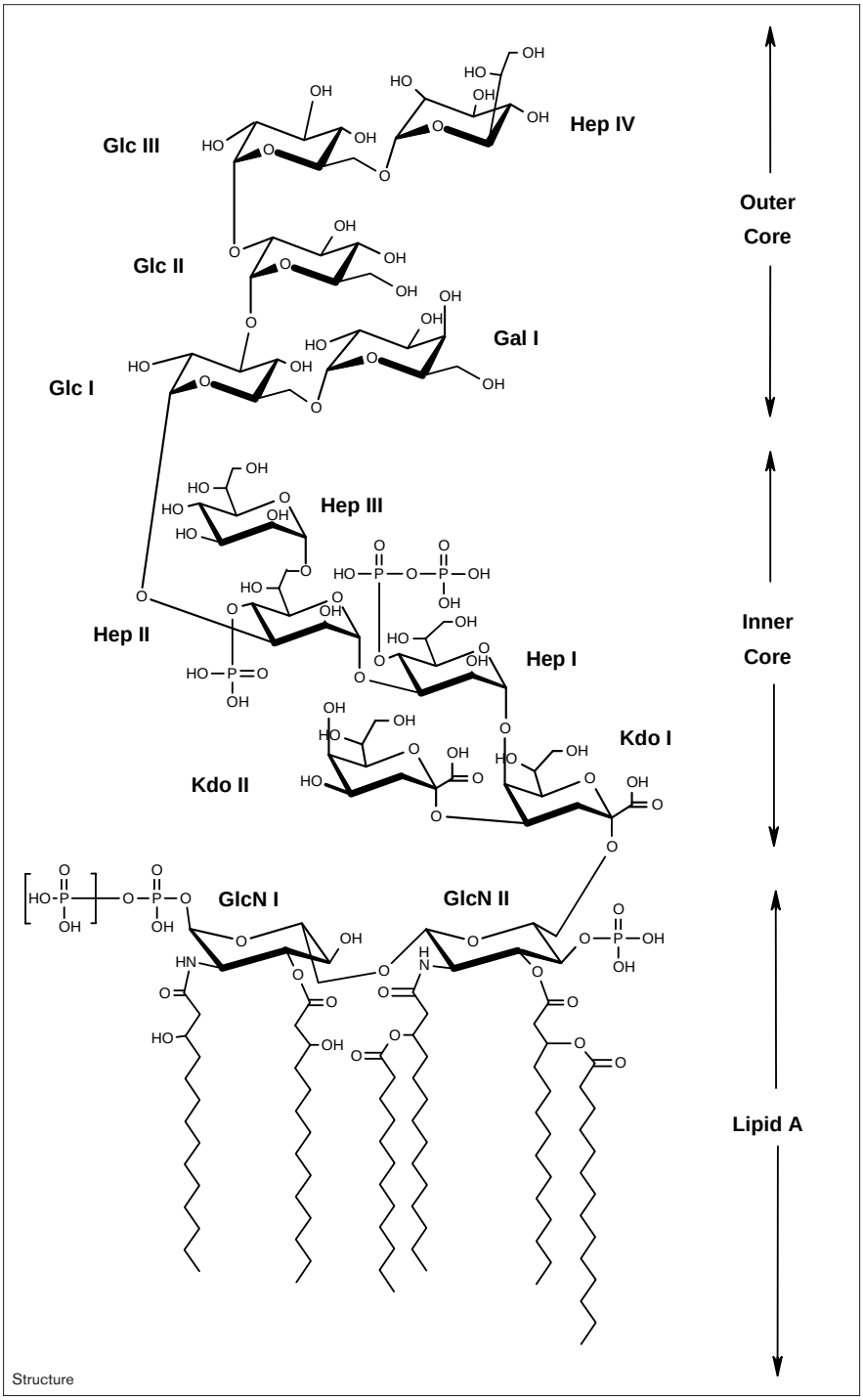

Chemical structure of *E. coli* K-12 LPS from strains AW740 and DL41 showing its three domains and their constituents. Enterobacterial lipid A is a phosphorylated 2-amino-2-deoxy-D-glucose (glucosamine) disaccharide. The two linked glucosamines (GlcN I and GlcN II) are bisphosphorylated at the *O*1-position of GlcN I and monophosphorylated at the *O*4′-position of GlcN II. The secondary phosphate position of the *O*1-diphosphate is not fully occupied (indicated with brackets). The glucosamine disaccharide is acylated (from left to right) at the 2- and 3-positions of GlcN I with 3-hydroxymyristatic [14:0(3-OH)] acid, and at the 2′- and 3′-positions of GlcN II with 14:0[3-*O*(C12:0)] and 14:0[3-*O*(C14:0)], respectively. The 3-hydroxymyristate group is partially disordered in both complexes and could not be modeled beyond the fourth carbon atom. The inner core comprises two 3-deoxy-D-*manno*-oct-2-ulopyranosonic acid groups (Kdo I and Kdo II), three L-*glycero*-D-*manno*-heptopyranose groups (Hep I, Hep II and Hep III) and phosphate residues. In AW740-LPS, Hep I is bisphosphorylated whereas in DL41-LPS, a 2-aminoethyl phosphate group is present. Hep II is monophosphorylated in both structures. The outer core of both LPS molecules consists of hexose moieties, including D-galactose (Gal), D-glucose (Glc) and a disordered fourth heptose group (Hep IV). Although Hep III, Hep IV and Glc III were chemically identified in both complexes, they could not be modeled. This figure was prepared using ISIS Draw.

[9]. The Gram-negative bacterium *E. coli* K-12 has defects in the gene cluster responsible for the biosynthesis of O antigen; strains AW740 and DL41 therefore synthesize a truncated ('rough') form of LPS consisting of lipid A and the core only, whereas wild-type *E. coli* expresses the complete ('smooth') form.

This paper details the molecular conformation of LPS and its interactions with surface residues of FhuA in the FhuA–LPS complex as obtained by compositional data, mass spectrometric analyses and crystallographic refinement, and reports a mode of protein–LPS interaction that appears to be shared by many LPS-binding proteins.

Results and discussion

Given the lack of detailed chemical information about the LPS molecules in our FhuA–LPS complexes and the limited resolution of our electron-density maps, we conducted a complete chemical analysis of LPS extracted from the OM of *E. coli* strains AW740 and DL41 and of LPS derived from purified FhuA–LPS preparations. This information was used to model the ambiguous regions of the LPS molecules in our crystal structures. Our compositional and detailed mass spectrometric analyses of LPS from OM extracts of both bacterial strains and from protein preparations used for crystallization (Figure 1) lead to complete crystallographic models of the LPS molecules (Figure 2).

Structural refinements of the two FhuA–LPS complexes provide improved crystallographic R factors compared with those reported in [7], and good matches to the electron-density maps (Figure 2c). For the FhuA–AW740-LPS complex, it was possible to complete the atomic model by including eight crystallographically visible glycerol and three detergent molecules. The temperature factors of all parts of the atomic models are at a high level; in both complex structures, average atomic B factors are around 66 Å^2 for the protein and lipid A, 70 Å^2 for the inner core and 96 Å^2 for the outer core of LPS. Detergent, glycerol (in the FhuA–AW740-LPS complex) and water molecules show average B factors around 90 Å^2, 90 Å^2 and 60 Å^2, respectively. Ferricrocin (in the FhuA–DL41-LPS–ferricrocin complex), at a B factor around 50 Å^2, is bound to the cork domain and together with parts of the β strands is the most rigid part of the complexes (at average B factors slightly less than 50 Å^2). Despite the high average B factors, the models reside in good electron density, with the exception of a few surface-exposed sidechains at some of the outer loops. Our models of FhuA closely match (root mean square deviations [rmsds] of 0.5 Å for Cα atoms, 1.0 Å for all atoms) those obtained in an independant study [10] from an LPS-free crystal form.

In the crystallographic structure, the LPS molecule is closely associated with the FhuA barrel, burying an accessible surface area of 1800 Å^2. Numerous van der Waals contacts with hydrophobic sidechains of FhuA fix all acyl chains of the bound LPS molecule, except for the 3-hydroxymyristate, in a highly ordered conformation, approximately parallel to the barrel axis (Figure 2a). In common with all OM proteins studied so far, FhuA has two girdles of aromatic residues that are 25 Å apart, extending into the lipid bilayer and marking the boundary of a cylindrical zone of hydrophobic residues on the barrel surface. These girdles were proposed to delineate the interface between the membrane lipids and the polar head groups of LPS. Indeed, we find the amide and ester bonds linking the acyl chains to the glucosamine disaccharide being situated slightly above the upper aromatic belt. In both FhuA–LPS complexes, the line connecting the O1 and O4′-phosphate moieties of lipid A is perpendicular to the barrel axis and thus parallel to the plane of the OM.

Figure 2

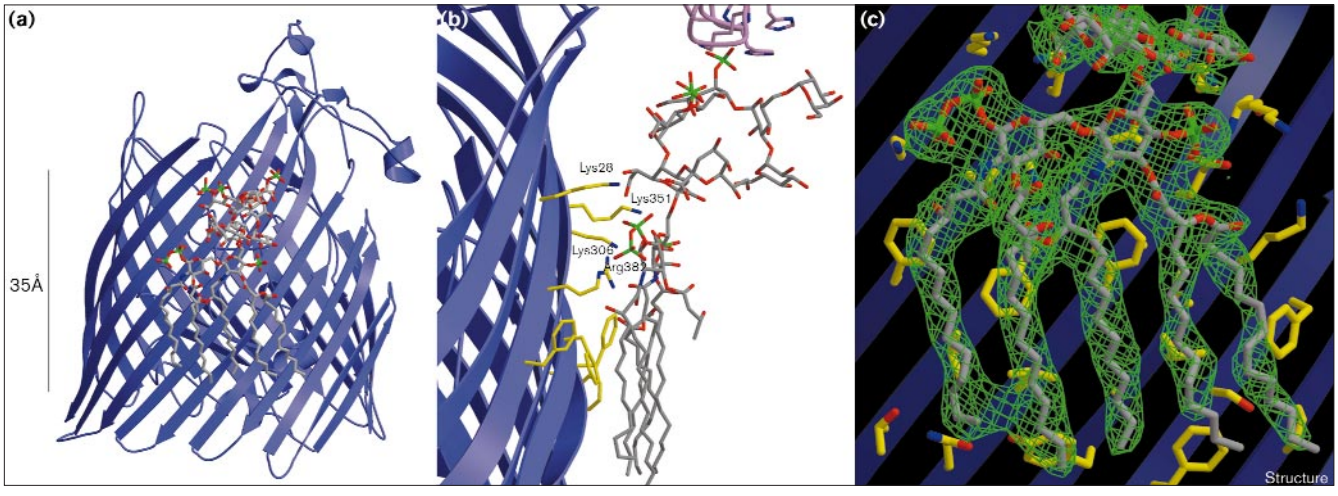

Crystal structure of the FhuA–LPS complex. **(a)** The FhuA–AW740-LPS complex in ribbon representation shows the placement of the LPS molecule in relation to the outer barrel surface of FhuA. The view is perpendicular to the barrel axis. **(b)** Close-up view perpendicular to the barrel axis. Selected sidechain residues of the upper aromatic girdle and those that comprise the LPS-binding motif (labeled) are colored yellow. The AW740-LPS molecule is represented as a stick model with oxygen atoms red, nitrogen atoms blue, phosphorous atoms green, and carbon atoms gray. The His-tag of a symmetry-related FhuA molecule (pink) forms a crystal contact with the phosphates of the inner core of LPS. **(c)** Electron density (obtained with a simulated-annealing omit calculation) at 2.1σ around lipid A of the FhuA–AW740-LPS complex. The view is the same as in (a). In all panels, the barrel surface of FhuA is colored blue. This figure and Figure 3 were prepared using MOLSCRIPT [21] and Raster3D [22].

The outer core bends away from the barrel axis and is in contact neither with the barrel nor with the external surface-exposed loops of FhuA (Figure 2b). The bend might be induced by a crystal contact between a phosphorylated heptose group of the inner core and the hexahistidine tag of a symmetry-related FhuA molecule.

Our findings are in general agreement with current models of the architecture of the OM [11]. The outer leaflet of the OM is the LPS monolayer, which contributes to the integrity of the Gram-negative cell envelope. Absence of O antigen does not alter the integrity of the OM [12] nor does absence of the outer core or the non-phosphorylated heptose residues of the inner core. Bacterial mutants with defects in the synthesis or incorporation of the phosphorylated heptose of the inner core (deep rough mutants) show hypersensitivity to lipophilic solutes. The phosphorylated heptose moieties of the inner core thus have an important role in stabilization of this part of the membrane.

In the OM of *E. coli*, electrostatic repulsions between adjacent, negatively charged LPS molecules are neutralized by divalent cations. Removal of these cations from the OM with chelating agents destabilizes the LPS monolayer by disrupting specific intermolecular LPS–LPS contacts [11]. The specific interaction of phosphates with positively charged groups on FhuA can serve as a model for the LPS–LPS interaction as promoted by divalent cations in the OM. Our finding of an alignment of the diglucosamine phosphate moieties in the plane of the OM is contrary to results based on small-angle X-ray scattering and molecular modeling [13]. The arrangement that we find offers an alternative mode of interaction between neighboring LPS molecules, predicting in-plane cross-linking of divalent cations and diglucosamine phosphates.

The innate immune response elicited against Gram-negative bacteria is not triggered by the intact OM, but by recognition of single LPS molecules, and involves specialized binding proteins and receptors [4,5]. Given the atomic details of the interaction between FhuA and LPS, it was our goal to identify the arrangement of residues that are conserved among LPS-binding proteins.

In the FhuA–LPS complex, 11 charged or polar residues interact with the negatively charged phosphates of the inner core and the diglucosamine backbone of lipid A (Table 1 and Figure 2). These residues are responsible for the tight binding of LPS to FhuA, and we hypothesized that they constitute a conserved motif in LPS-binding proteins. They involve short discontinuous segments found on β strands 7–11. Most of the favourable interactions are contributed by a cluster of eight positively charged residues on the surface of the barrel, which interact by hydrogen bonding at distances around 3 Å, or electrostatically (Lys306 and Arg424) at longer distances. The electrostatic Coulomb potential of the latter residues might appear to provide little contribution to the overall binding enthalpy, however, it falls off only inversely proportional to distance, and their presence might be important for charge compensation in the binding site. Crystallographically visible water molecules, which would tend to weaken electrostatic interactions, are not found between the two residues and LPS.

Using a conventional sequence-based search with the LPS-interacting residues on FhuA, we did not identify

Table 1

Charged or polar FhuA–LPS interactions.

Residue– Atom	Location	Distance (Å)	Type of interaction
Glu304 OE1	β7	2.7	Hydrogen bond with the O3 atom of the 4′-phosphate
Glu304 OE2		3.4	Hydrogen bond with the O3 atom of the 4′-phosphate
Lys306 NZ*	β7	6.9	Electrostatic interactions with the 4′-phosphate
Lys351 NZ*	β8	2.5	Hydrogen bond with the O4 atom of the 4′-phosphate
Gln353 OE1	β8	3.7	Hydrogen bond with the O8 atom of Kdo I
Arg382 NH1*	β9	2.7	Hydrogen bond with the O2-carbonyl atom of the 3′-lauristate residue
Arg382 NH2*		3.6	Hydrogen bond with the O5 atom of GlcN I
Arg384 NE	β9	3.5	Hydrogen bond with the O7 atom of Kdo I
Arg384 NH1		3.3	Hydrogen bond with the O3 atom of the 1-phosphate
Arg384 NH2		2.9	Hydrogen bond with the O1B atom of Kdo II
Asp386 OD2	β9	2.6	Hydrogen bond with the O7 atom of Kdo I
Arg424 NH1	β10	6.6	Electrostatic interactions with the O2 atom of Hep I
Lys428 NZ*	β10	3.1	Hydrogen bond with the O3 atom of the 1-phosphate
Lys430 NZ	β10	2.4	Hydrogen bond with the O2 atom of the secondary 1-phosphate
Arg463 NH1	β11	2.8	Hydrogen bond with the O6 atom of Hep I
Arg463 NH2		2.6	Hydrogen bond with the O5 atom of Hep I

Listed are the residues and atoms on FhuA, their location on the β strands of FhuA, distance and type of interaction. 12 additional sidechain residues form non-specific van der Waals contacts with LPS atoms (data not shown). Residues that form the conserved LPS-binding motif are marked with an asterisk.

Figure 3

Stereoview of the FhuA LPS-binding site, perpendicular to the barrel axis. Selected FhuA sidechain residues that form specific and non-specific van der Waals contacts with the LPS molecule are colored in yellow. The outer barrel surface of FhuA is shown in blue. Those residues that compose the conserved LPS-binding motif are marked with an asterisk. The AW740-LPS molecule is shown as a stick model (oxygen atoms, red; nitrogen atoms, blue; phosphorous atoms, green; carbon atoms, gray).

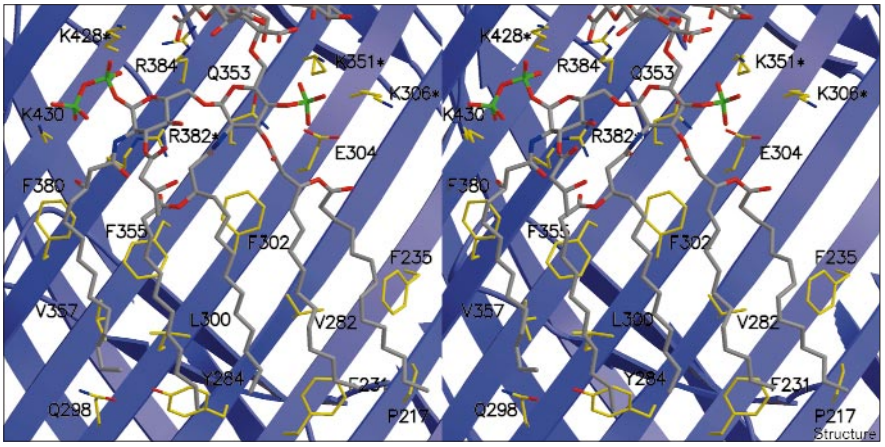

similar LPS-binding motifs in sequence databases. Furthermore, no other structures of protein–LPS complexes are available for comparison with the FhuA–LPS complex. Therefore, we designed and utilized a structure-based search strategy to identify in the Protein Data Bank (PDB) residue subsets that are structurally similar to those of FhuA's LPS-binding residues.

Any sequence- or structure-based search strategy must find a compromise between high specificity (which avoids false positive matches), and high sensitivity (which avoids false negatives). The objective is to produce a high number of true matches on a low background of false positives. The 'proper' subset of residues detects those proteins that are known to interact specifically with LPS, but

Table 2

LPS-binding residues identified by structural searches.

Protein	PDB code	Superimposed residues				Rmsd (Å)
		Lys306	**Lys351**	**Arg382**	**Lys428**	
BPI*	1bp1	Lys42	Arg48	Lys92	Lys99	0.88
Lactoferrin† N-terminal lobe	1bx1	Arg24	Arg27	Arg2	Arg4	1.47
C-terminal lobe		Lys359	Arg356	Lys633	Lys637	1.25
Lysozyme‡ Human	1jkc	Arg113	Arg107	Lys97	Arg21	1.38
C-type	135l	Lys96	Lys97	Arg61	Lys73	1.45
G-type	1hhl	Arg14	Lys13	Lys125	Arg121	1.43
V-type	145l	Arg148	Lys147	Arg137	Lys135	1.07
LALF§	–	Arg41	Arg40	Lys64	Lys47	1.43

LPS-binding proteins and their LPS-binding residues identified by a structural search of the PDB. Rmsd is after superposition with equivalent residues in the LPS-binding motif of FhuA (bold). *The bactericidal/permeability-increasing (BPI) protein [23–26] produced by polymorphonuclear neutrophils and targeted against endocytosed bacteria, has a functional role in LPS-binding and LPS detoxification. The crystallographic structure of BPI consists of two similar, extended domains. The four BPI residues are located at the distal tip of the N-terminal domain and a functional role in LPS-binding and LPS detoxification has been assigned to these highly conserved residues. Peptides derived from residues 17–45 and residues 65–99 of BPI inhibit the LPS-induced inflammatory response. †Lactoferrin [27–31], an iron-binding glycoprotein found at mucosal surfaces and in biological fluids, is released from neutrophil granules during the LPS-induced inflammatory response. The crystallographic structure of human lactoferrin is composed of two related globular lobes. Two spatially distinct putative LPS-binding sites have been identified for lactoferrin: residues 2–4 in combination with residues 28–34 form the N-terminal high-affinity LPS-binding site. A second low-affinity LPS-binding site is present in the C-terminal lobe. Synthetic peptides containing residues 28–34 of lactoferrin are bactericidal against Gram-negative bacteria. ‡Lysozyme [31,32], a cationic protein found in leukocyte polymorphonuclear granules, reduces the immunostimulatory activities of LPS. Detailed information about specific LPS–lysozyme interactions is not available. The crystallographic structures of several different lysozyme types have been solved: human lysozyme [33], hen egg-white lysoyzme (C-type [34]), goose egg-white lysozyme (G-type [35]), and bacteriophage T4 lysozyme (V-type [36]). Although these proteins share a common fold, sequence comparisons between lysozyme types reveal no significant similarity. §The *Limulus* antibacterial and anti-LPS factor (LALF) [37–39] inhibits the LPS-induced coagulation cascade by binding LPS and neutralizing its endotoxic effects. The crystallographic structure of LALF contains a cluster of positively charged residues found on an amphipathic loop and on the adjacent residues of the basic face of LALF. Some of these residues have been previously proposed, but not demonstrated to be involved in LPS binding. Synthetic cyclic peptides derived from residues 36–45 of LALF have been shown to bind and inhibit the LPS-induced immune response.

avoids matches with proteins that do not interact *in vivo* with LPS. Proteins with an LPS-binding motif similar to that on FhuA are expected to yield rmsds below 1.5 Å for those residues that form a common LPS-binding motif. This value corresponds to an average bond distance between atoms and thus ensures that chemically equivalent atoms of superimposed motifs occupy equivalent positions in space.

We constrained the structure-based searches to the eight positively charged (arginine or lysine) residues from Table 1. Our rationale for this choice is the fact that positively charged residues are *a priori* more suitable for binding LPS, which has negatively charged phosphates and a number of carbohydrates with negative partial charges. Furthermore, positive charges are experimentally found to be a necessary requirement for the interaction of LPS with its natural environment, the outer membrane. Using all subsets consisting of five, six, seven or the complete set of these eight residues as search templates, no structural homologs with rmsds <1.5 Å were identified in the PDB. Searches conducted with three-residue subsets detected a high number of non-specific matches at rmsds <1.5 Å. All except one of the four-residue subsets detected a small number of matches in the PDB. That exception is the four-residue search template of FhuA residues Lys306, Lys351, Arg382 and Lys428, which identified a much larger group of matches at low rmsds. Three of these four residues form strong hydrogen bonds with the phosphates of lipid A (Table 1 and Figure 3). We therefore denote these four FhuA residues as the LPS-binding motif. Indeed, lipid A, the most conserved component of LPS, has a specific stereochemistry because of multiple asymmetric carbon atoms, and has been implicated in recognition by high-affinity LPS-binding proteins [8].

Our structural search of the PDB using this LPS-binding motif identified membrane-associated proteins, bacterial toxins, colicins and ribonucleotide-binding proteins. Among the proteins identified using this subset of four residues are all those proteins (bactericidal/permeability-increasing protein BPI, lactoferrin, lysozyme, and *Limulus* anti-LPS factor LALF) in the PDB that are known to bind LPS specifically and that mediate the LPS-induced immune response. In all cases, the proposed LPS-binding sites found on these proteins are consistent with functional and mutational data (Table 2). All residues of these LPS-binding sites are surface-exposed and docking of LPS to these proteins is possible without steric clashes. The four-residue subset thus represents an LPS-binding motif, which is remarkably conserved in proteins of procaryotic and eucaryotic origin.

Our data support the proposal [4,5] that a conserved mode of LPS recognition by LPS-binding proteins is involved in the innate immune response. A consequence of this mechanism is that increased bacterial virulence *in vivo* should result from LPS modifications, as has been observed [14]. Although the structural scaffold of the four-residue motif, which we identify, appears to be necessary for LPS binding, our findings do not currently allow us to investigate the individual roles of the four residues. Their respective importance, as well as the contribution of other residues in the individual binding sites of FhuA and other LPS-binding proteins, remains to be established using site-directed mutagenesis. With respect to the choice of residues from Table 1 for the superposition searches, we find that the exclusive use of positively charged residues appears justified by the fact that neither in BPI, nor in lactoferrin, lysozyme or LALF do we find residues equivalent to the residues of FhuA: Glu394, Gln353 or Asp386.

For those structurally known proteins identified by our search, as well as for new crystallographic structures, the four-residue LPS-binding motif of FhuA might readily be used both to map the LPS-binding site, and to model a complex with LPS. Such models might facilitate the rational design of proteins with modified LPS-binding properties.

Biological implications

Lipopolysaccharide (LPS) is the major component of the outer membrane of Gram-negative bacteria; as such, it is an important activator of the innate immune response. Its three-dimensional structure, alone or in complex with a protein, has hitherto not been elucidated in atomic detail. This work describes the crystallographic structure of its complex with FhuA, a ferric hydroxamate uptake receptor on the surface of *Escherichia coli*. The lipid A portion of LPS, which is its most invariant part, interacts specifically with positively charged residues on the outer surface of the β-barrel of FhuA.

A search through the database of known protein structures, using subsets of those residues identified in the LPS binding site of FhuA, identifies four residues the arrangement of which on the surface of known LPS-binding proteins is conserved. These residues appear to be the crucial elements of pattern recognition in the innate immune response.

The following applications of this knowledge are feasible. Known LPS-binding proteins might be altered for their binding properties: they could be engineered for higher or lower LPS-binding affinity. Recombinant proteins that compete with naturally occurring LPS-binding proteins and that lack immunostimulatory activities will be advantageous in the treatment of bacterial sepsis. Novel bactericidal proteins or peptides might be designed [15] to intercalate into the outer membrane by their binding to lipid A. Such binding would increase the

permeability of the outer membrane and compromise its protective effect, and thereby kill bacterial cells.

Materials and methods

Chemical analysis

Compositional analysis of LPS extracted from the outer membranes of *E. coli* strains (AW740 and DL41), performed according to published methods [16], identified constituents and their approximate molar ratios: Gal (1.0/1.0), Glc (2.6/2.5), GlcN (1.9/1.9), Hep (3.1/2.9), Kdo (2.0/1.9), rhamnose (trace amounts/0.3), phosphate (4.4/5.6) and 2-aminoethanol (0.2/0.6). The relatively low Hep content is most probably because of the phosphate substitutions linked to the Hep residues, which further stabilize their glycosidic linkages. The GlcN content demonstrated that there are no additional GlcN substitutions at the nonreducing terminus of the core.

Mass spectrometry

Matrix-assisted laser desorption ionization mass spectrometry including post source decay analysis were performed with the two-stage reflectron time-of-flight mass analyzer Bruker-Reflex III (details of the applied methods are described in [17]). Spectra from membrane-extracted AW740-LPS and DL41-LPS displayed the expected heterogeneity for *E. coli* K-12 LPS (data not shown). A series of molecular ions differing in their phosphate and 2-aminoethyl phosphate substitutions were identified as various combinations of Kdo, Hep, hexose (Gal and Glc) and lipid A residues. The most abundant core oligosaccharide in both LPS extracts consists of two Kdo residues, four Hep residues, and four hexose residues and up to four phosphate residues in nonstoichiometric amounts. In contrast to AW740-LPS, DL41-LPS showed further heterogeneity arising from additional 2-aminoethyl phosphate groups.

X-ray crystallography

The structure of the FhuA–AW740-LPS complex was solved and initially refined at 2.50 Å resolution [7]. Following additional rounds of model building using the program O [18] and structural refinement with CNS [19], the final model now contains residues 19–725, one LPS, three detergent (dimethyldecylamine-*N*-oxide, DDAO), eight glycerol and 244 water molecules (R_{cryst} 22.1% and R_{free} 27.1%).

This structure was used in the refinement of FhuA–DL41-LPS–ferricrocin complex at 2.70 Å resolution. The final model contains residues 19–725, one LPS, one ferricrocin and 152 water molecules (R_{cryst} 23.1% and R_{free} 27.6%). Because of the lower resolution, glycerol or detergent molecules were not included in the model.

All residues of both complexes except Asp454, which is in a periplasmic turn of high mobility, reside in generously allowed regions of the Ramachandran plot; 85% (FhuA–AW740-LPS) and 82% (FhuA–DL41-LPS–ferricrocin) of the residues are in most favoured regions.

The main differences between these models, compared with those reported previously [7], are in the conformation and composition of the LPS molecules, and the modelling of detergent and glycerol molecules in the case of the FhuA–AW740-LPS crystals. Throughout this article we use the residue numbering of the wild-type FhuA sequence. The coordinates submitted to the PDB (1qff, FhuA–DL41-LPS–ferricrocin and 1qfg, FhuA–AW740-LPS) differ in their numbering because of the insertion of 11 residues of the His-tag after Pro405 (the sequence in this region has been corrected with respect to that given in [7]).

Structural searches

After constructing a database from the PDB (status on January 25th, 1999) the program SPASM [20] was employed to superimpose subsets of the eight positively charged residues LPS-binding residues (Table 1) upon all deposited crystallographic protein structures. Motivated by a comparison of the LPS-binding site of our FhuA models and the LPS-free FhuA from Locher *et al.* [10], the sidechains of all residues were truncated beyond the Cγ atom because the conformation of those residues that compose the LPS-binding motif can be expected to differ in the LPS-bound and the LPS-free form. SPASM uses a fast search procedure based on differences between atomic positions. Neither chain directionality nor gap size constraints were imposed, and only Lys–Arg substitutions were permitted. The eight-residue set, and all seven-residue (8 combinations), six-residue (28 combinations), five-residue (56 combinations), four-residue (70 combinations), and three-residue (56 combinations) subsets were systematically assessed. This procedure mimics the properties of a sequence-based search which permits insertions and deletions with respect to a given sequence motif.

Accession numbers

The coordinates for FhuA–DL41-LPS–ferricrocin and FhuA–AW140-LPS were submitted to the PDB with accession codes 1qff and 1qfg, respectively.

Acknowledgements

We gratefully acknowledge H Brade for Western blots and for providing anti-*E. coli* K-12 antibodies; A Hoess for providing LALF coordinates; H Lüthje and A Müller for technical assistance; DM Allan, MA Arbing, MG Baines, M Cygler and D Malo for reading the manuscript; and M Kastowsky for ISIS draw files. This work was supported by the Deutsche Forschungsgemeinschaft (WW), by the Medical Research Council, Canada (JWC) and by a NATO International Collaborative Research Grant. ADF is recipient of a Deutscher Akademischer Austauschdienst Grant for Study and Research and a Medical Research Council of Canada Doctoral Research Award.

References

1. Mamat, U., Seydel, U., Grimmecke, D., Holst, O. & Rietschel, E.T. (1999). *Comprehensive Natural Products Chemistry.* (Pinto, M. ed), pp.179-239, Elsevier Science, Amsterdam.
2. Holst, O. (1999). *Endotoxin in Health and Disease.* (Brade, H., Morrison, D.C., Opal, S. & Vogel, S. eds), pp.115-154, Marcel Dekker Inc., New York
3. Zähringer, U., Lindner, B. & Rietschel, E.T. (1999). *Endotoxin in Health and Disease.* (Brade, H., Morrison, D.C., Opal, S. & Vogel, S. eds), pp. 93-114, Marcel Dekker Inc., New York.
4. Medzhitov, R. & Janeway, C.A Jr. (1997). Innate immunity: the virtues of a nonclonal system of recognition. *Cell* **91**, 295-298.
5. Hoffmann, J.A., Kaftatos, F.C., Janeway, C.A Jr. & Ezekowitz, R.A.B. (1999). Phylogenetic perspectives in innate immunity. *Science* **284**, 1313-1318.
6. Moeck, G.S. & Coulton, J.W. (1998). TonB-dependent iron acquisition: mechanisms of siderophore-mediated active transport. *Mol. Microbiol.* **28**, 675-681.
7. Ferguson, A.D., Hofmann, E., Coulton, J.W., Diederichs, K. & Welte, W. (1998). Siderophore-mediated iron transport: crystal structure of FhuA with bound lipopolysaccharide. *Science* **282**, 2215-2220.
8. Raetz, C.R.H. (1996). *Escherichia coli* and *Salmonella*, Cellular and Molecular Biology. (Neidhardt, F.C. ed.), pp. 1035-1063, American Society for Microbiology Press, Washington, DC.
9. Brandenburg, K., *et al.*, & Rietschel, E.T. (1996). Conformation of lipid A, the endotoxic center of bacterial lipopolysaccharide. *J. Endotoxin Res.* **3**, 173-178.
10. Locher, K.P., *et al.*, & Moras, D. (1998). Transmembrane signaling across the ligand-gated FhuA receptor: crystal structures of free and ferrichrome-bound states reveal allosteric changes. *Cell* **95**, 771-778.
11. Nikaido, H. (1996). *Escherichia coli* and *Salmonella*, Cellular and Molecular Biology. (Neidhardt, F.C. ed.), pp. 29-47, American Society for Microbiology Press, Washington, DC.
12. Cygler, M., Rose D.R. & Bundle, D.R. (1991). Recognition of a cell-surface oligosaccharide of pathogenic *Salmonella* by an antibody Fab fragment. *Science* **253**, 442-445.
13. Kastowsky, M., Sabisch, A., Gutberlet, T. & Bradaczek, H. (1991). Molecular modelling of bacterial deep rough mutant lipopolysaccharide of *Escherichia coli*. *Eur. J. Biochem.* **197**, 707-716.
14. Guo, L., *et al.*, & Miller, S.I. (1998). Lipid A acylation and bacterial resistance against vertebrate antimicrobial peptides. *Cell* **95**, 189-198.
15. Hwang, P.M. & Vogel, H.J. (1998). Structure–function relationships of antimicrobial peptides. *Biochem. Cell Biol.* **76**, 235-246.

16. Kaca, W., de Jongh-Leuveninck, J., Zähringer, U., Rietschel, E. T., Brade, H., Verhoef, J. & Sinnwell, V. (1988). Isolation and chemical analysis of 7-*O*-(2-amino-2-deoxy-alpha-D-glucopyranosyl)-L-*glycero*-D-*manno*-heptose. *Carbohydrate Res.* **179**, 289-299.
17. Lindner, B. (2000). *Methods in Molecular Biology: Bacterial Toxins Methods and Protocols.* (Holst, O. ed.), pp. 311-325, Humana Press Inc., Totowa, NJ.
18. Jones, T.A., Zou, J.Y., Cowan, S.W. & Kjeldgaard, G. (1991). Improved methods for building protein models in electron density maps and the location of errors in these models. *Acta Crystallogr. A* **47**, 110-119.
19. Brünger, A.T., *et al.*, & Warren, G.L. (1998). Crystallography & NMR system: A new software suite for macromolecular structure determination. *Acta Crystallogr. D* **54**, 905-921.
20. Kleywegt, G. (1999). Recognition of spatial motifs in protein structures. *J. Mol. Biol.* **285**, 1887-1897.
21. Kraulis, P. (1991). MOLSCRIPT: a program to produce both detailed and schematic plots of protein structures. *J. Appl. Crystallogr.* **24**, 946-950.
22. Merrit, E.A. & Bacon, D.J. (1997). Raster3D photorealistic molecular graphics. *Methods Enzymol.* **277**, 505-524.
23. Little, R.G., Kelner, D.N., Lim, E., Burke, D.J. & Conlon, P.J. (1994). Functional domains of recombinant bactericidal/permeability increasing protein (rBPI23). *J. Biol. Chem.* **269**, 1865-1872.
24. Beamer, L.J., Carroll, S.F. & Eisenberg, D. (1998). The BPI/LBP family of proteins: a structural analysis of conserved regions. *Protein Sci.* **7**, 906-914.
25. Taylor, A.H., *et al.*, Ghrayeb, J. (1995). Lipopolysaccharide (LPS) neutralizing peptides reveal a lipid A binding site of LPS binding protein. *J. Biol. Chem.* **270**, 17934-17938.
26. Lamping, N., *et al.*, & Schumann, R.R. (1996). Effects of site-directed mutagenesis of basic residues (Arg94, Lys95, Lys99) of lipopolysaccharide (LPS)-binding protein on binding and transfer of LPS and subsequent immune cell activation. *J. Immunol.* **157**, 4648-4656.
27. Appelmelk, J., *et al.*, & Nuijens, J.H. (1994). Lactoferrin is a lipid A binding protein. *Infect. Immun.* **62**, 2628-2632.
28. Anderson, B.F., Baker, H.M., Norris, G.E., Rice, D.W. & Baker, E.N. (1989). Structure of human lactoferrin: Crystallographic structure analysis and refinement at 2.8 Å resolution. *J. Mol. Biol.* **209**, 711-734.
29. Van Berkel, P.H.C., et al., & Nuijens, J.H. (1997). N-terminal stretch Arg2, Arg3, Arg4 and Arg5 of human lactoferrin is essential for binding to heparin, bacterial lipopolysaccharide, human lysozyme and DNA. *Biochem. J.* **328**, 145-151.
30. Elass-Rochard, E., *et al.*, & Spik, G. (1998). Lactoferrin inhibits the endotoxin interaction with CD14 by competition with the lipopolysaccharide-binding protein. *Infect. Immun.* **66**, 486-491.
31. Odell, E.W., Sarra, R., Foxworthy, M., Chapple, D.S. & Evans, R.W. (1996). Antibacterial activity of peptides homologous to a loop region in human lactoferrin. *FEBS Lett.* **382**, 175-178.
32. Brandenburg, K., Koch, M.H.J. & Seydel, U. (1998). Biophysical characterisation of lysozyme binding to LPS Re and lipid A. *Eur. J. Biochem.* **258**, 686-695.
33. Artymiuk, P.J. & Blake, C.C.F. (1981). Refinement of human lysozyme at 1.5 Å resolution. Analysis of nonbonded and hydrogen-bond interactions. *J. Mol. Biol.* **152**, 733-762.
34. Blake, C.C.F., *et al.*, Sarma, V.R. (1965). Structure of hen egg-white lysozyme. *Nature* **206**, 757-761.
35. Grütter, M.G., Weaver, L.H. & Matthews, B.W. (1983). Goose lysozyme structure: an evolutionary link between hen and bacteriophage lysozymes? *Nature* **303**, 828-831.
36. Matthews, B.W. & Remington, S.J. (1974). The three-dimensional structure of the lysozyme from bacteriophage T4. *Proc. Natl Acad. Sci. USA* **71**, 4178-4182.
37. Warren, H.S., *et al.*, & Novitsky, T.J. (1992). Binding and neutralization of endotoxin by Limulus antilipopolysaccharide factor. *Infect. Immun.* **60**, 2506-2513.
38. Hoess, A., Watson, S., Siber, G.R. & Liddington, R. (1993). Crystal structure of an endotoxin-neutralizing protein from the horseshoe crab, *Limulus* anti-LPS factor, at 1.5 Å resolution. *EMBO J.* **12**, 3351-3356.
39. Ried, C., *et al.*, & Hoess, A. (1996). High affinity endotoxin-binding and neutralizing peptides based on the crystals structure of recombinant Limulus anti-lipopolysaccharide factor. *J. Biol. Chem.* **271**, 28120-28127.

Because *Structure with Folding & Design* operates a 'Continuous Publication System' for Research Papers, this paper has been published on the internet before being printed (accessed from http://biomednet.com/cbiology/str). For further information, see the explanation on the contents page.